Table S1. The parameters used to construct the Comsol model that was used to predict the steady state O_2 concentration distribution in the vLAMPS model as a function of media flow rate.

Parameters	Symbol	Value	Units
O_2 consumption rate of hepatocytes	V_{max}	0.425	nmol/s/10^6 cells
Michaelis constant (O_2 consumption) of hepatocytes	K_m	3.5	mmHg
Diffusion coefficient of O_2 in media	D_m	3.35×10^{-9}	m^2/s
O_2 concentration in the influx media	c_{o2}	0.17075	mol/m^3
Porosity of the ECM & cell layer	ε_c	0.045	N/A
Diffusion coefficient of O_2 in the ECM & cell layer	D_c	3.018×10^{-11}	m^2/s
Porosity of the PET membrane	ε_p	0.057	N/A
Diffusion coefficient of O_2 in the PET membrane	D_p	1.0×10^{-11}	m^2/s

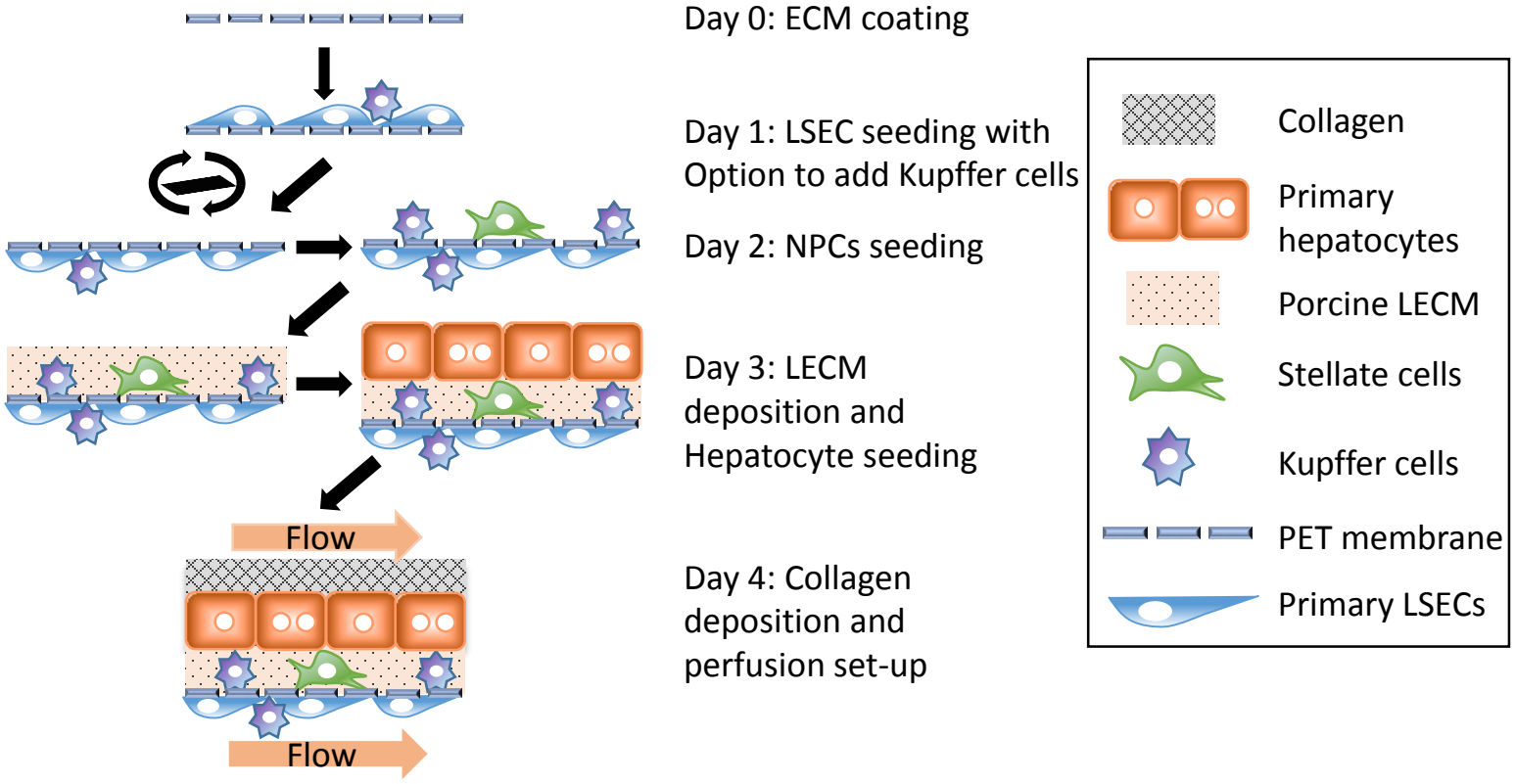

Fig S1. The sequential cell seeding process reconstitutes the liver sinusoid structure on the intermediate layer. After ECM coating (day 0), LSECs were seeded on the bottom side of the PET membrane (day 1) with the option to also add Kupffer cells. On day 2 HSCs (LX-2 human stellate cell line) and Kupffer cells (differentiated from THP-1 monoblast cell line) were seeded on the other side of the membrane. After the deposition of a thin LECM layer mimicking the space of Disse, human primary hepatocytes were seeded on day 3. With a protective collagen layer on top of the hepatocytes, the intermediate layers were assembled into the chip holder and perfusion was set-up on assembly day 4 (experiment day 0).

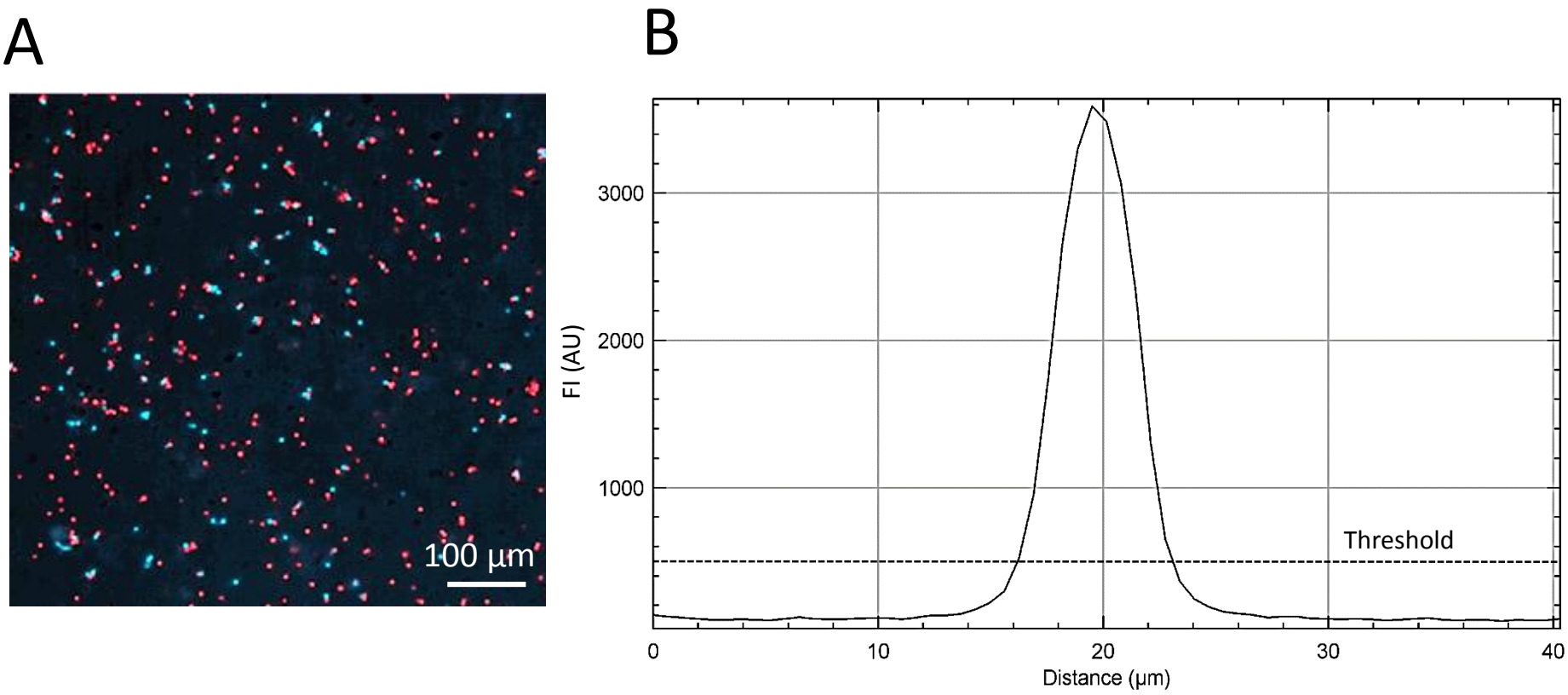

Fig S2. (A) A representative fluorescence image of oxygen sensitive beads (red) and insensitive beads (blue) from one region of interest (ROI) within the vLAMPS. (B) The intensity profile of one oxygen sensitive bead. The intensity threshold for segmentation of beads was set at 500 arbitrary fluorescence intensity units (AU).

Simulation of oxygen concentration (%)

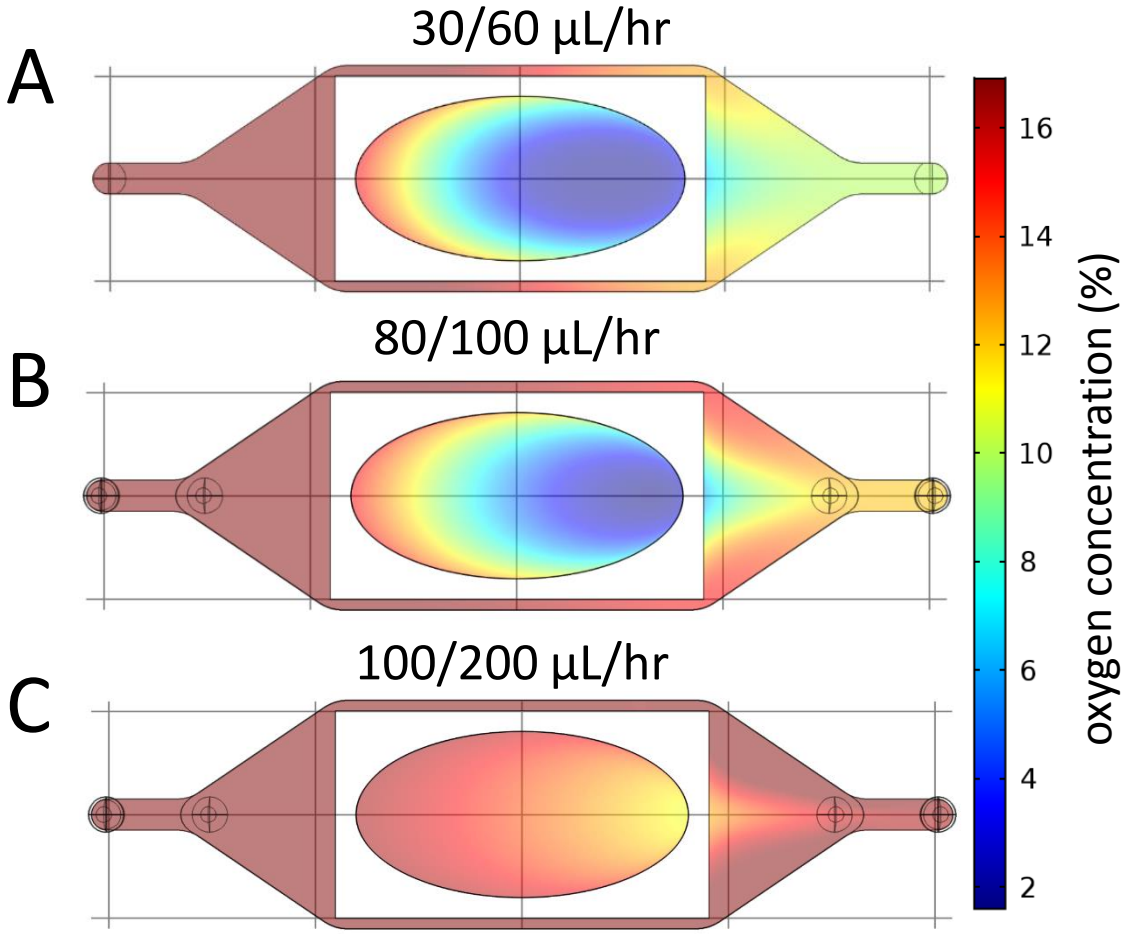

Fig S3. The oxygen concentration (%) under different flow rates was simulated in Comsol. (A) A mostly zone 3 (oxygen poor) domain was created within a single chip under the flow rate of 30/60 µL/hr in the hepatic/vascular channel. (B) Using flow rates of 80/100 µL/hr, an oxygen tension gradient is generated that includes all 3 zones distributed across the hepatocyte chamber. (C) To generate a mostly zone 1 (oxygen rich) domain within a single chip, the flow rate was increased to 100/200 µL/hr.

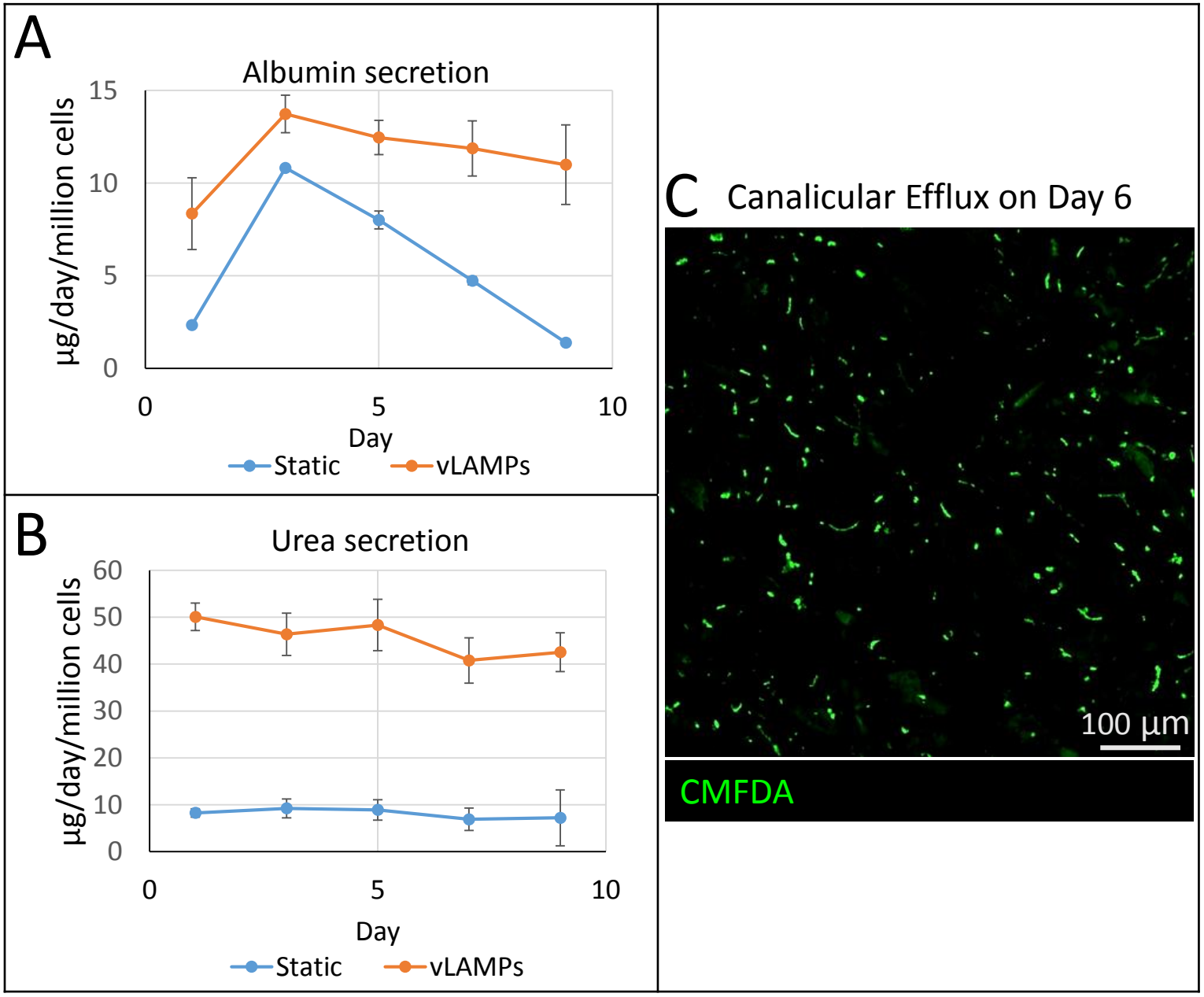

Fig S4. Demonstrations of liver functions in the vLAMPS. (A) Albumin and (B) Urea secretions were stable and elevated relative to static cultures. (C) Image from Zone 1 showing canalicular accumulation of CMFDA on Day 6, indicating active bile transporters. No quantitative difference was identified between zones 1 and 3.

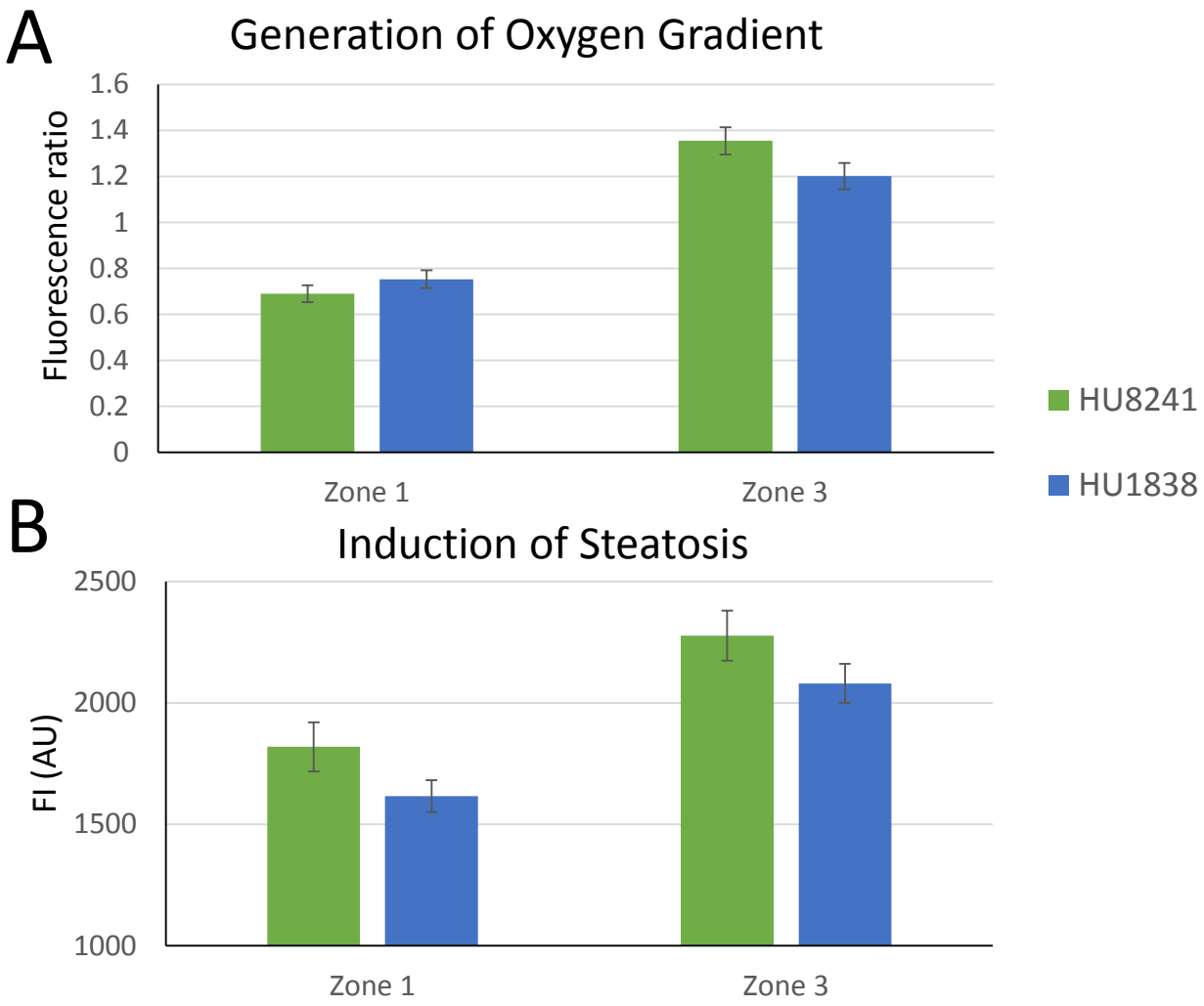

Fig S5. Comparison of Two Lots of Primary Human Hepatocytes in the vLAMPS. (A) Measurement of the oxygen tension using FI ratio with oxygen sensitive and insensitive beads in zones 1 & 3. The oxygen tensions generated by a second lot of hepatocytes (HU8241, green) are not significantly different than the lot used in this study (HU1838, blue) (p-value 0.26 and 0.08 for zone 1 and zone 3, respectively). (B) Both lots exhibited a 25-28% increase in steatosis in zone 3 vs zone 1, and there was no significant difference between lots (p-value 0.14 and 0.30 for zone 1 and zone 3, respectively). P-values based on a two-tailed t-test.

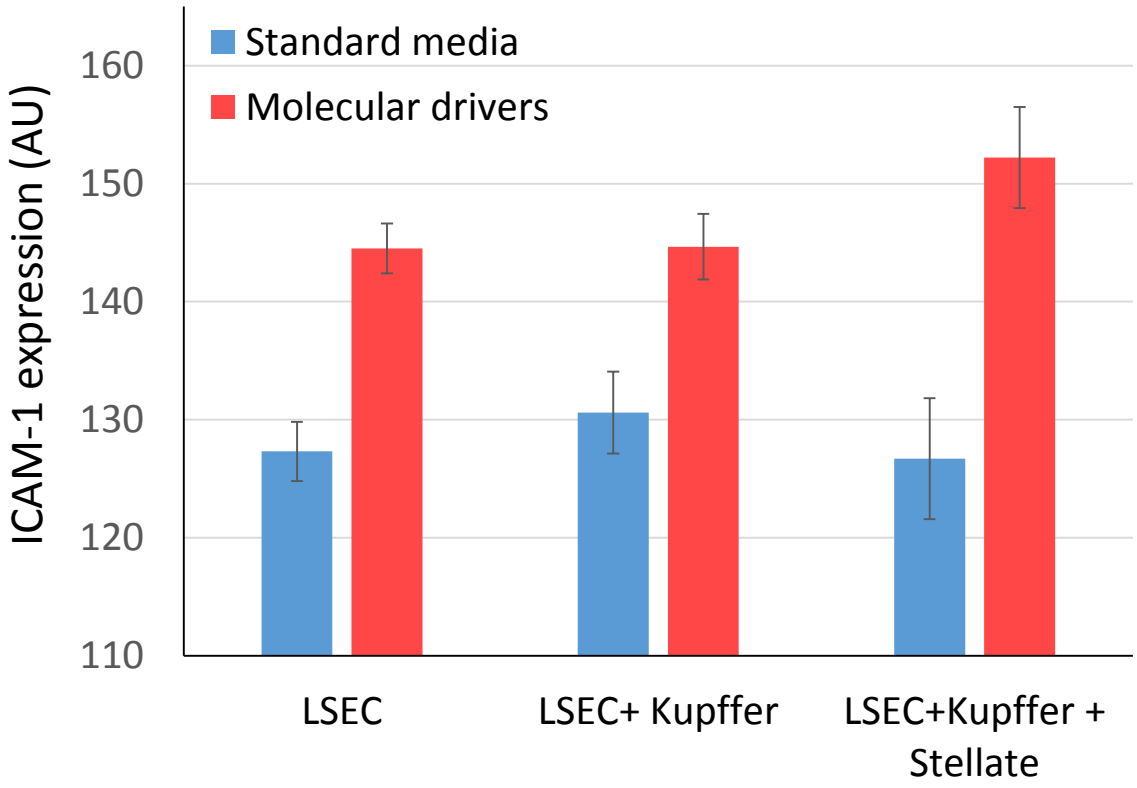

Fig S6. Activation of LSECs with molecular drivers of NAFLD that includes LPS, EGF and TGF-β. (A) Increased ICAM-1 expression of LSECs in response to the stimulation of molecular drivers over 16 hr. The expressed ICAM-1 level is slightly increased when all NPCs were present, indicating their individual contributions to the inflammatory response.

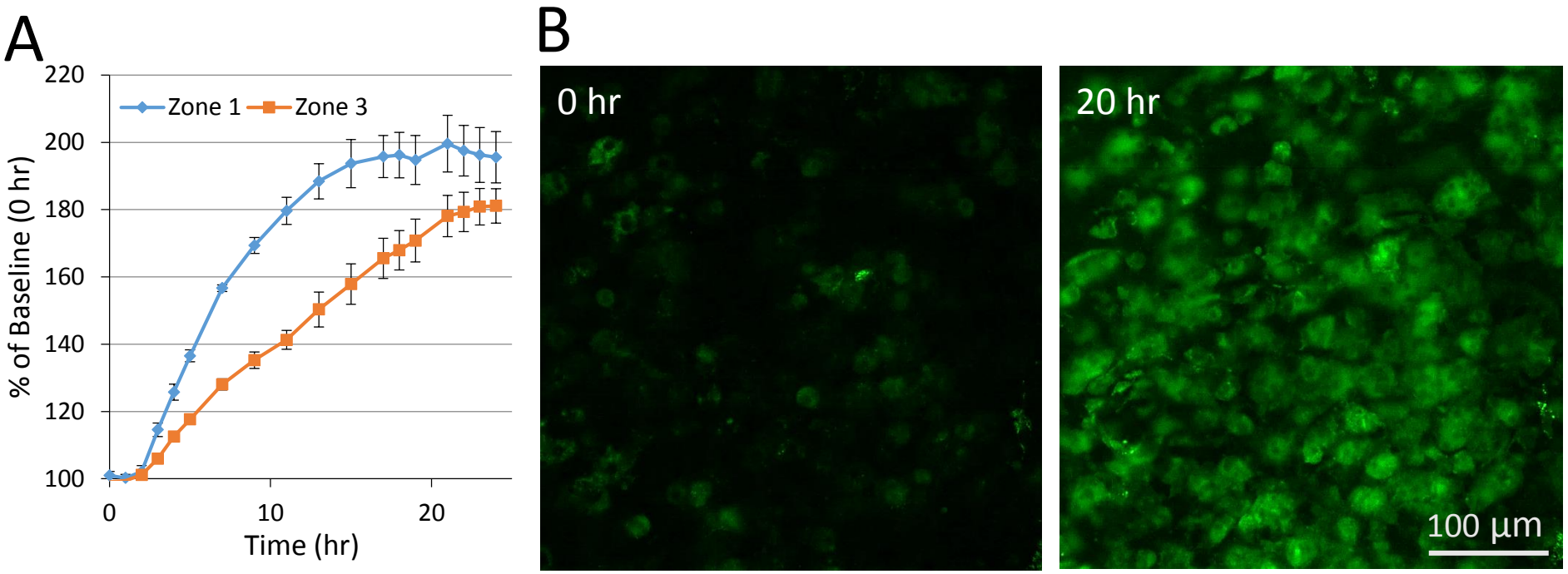

Fig S7. Live imaging of a reactive oxygen species (ROS) biosensor in hepatocytes in the vLAMPS. Menadione (100 µM) was perfused for 24 hr (29). (A) Time dependent increase in ROS measured as percent of total fluorescence intensity at T=0. The ROS production rate is higher in zone 1 than zone 3. (B) Representative images of the ROS biosensor signal at 0 hr and 20 hr.